“ALEXANDRU IOAN CUZA” UNIVERSITY OF IASI
FACULTY OF CHEMISTRY
DOCTORAL SCHOOL OF CHEMISTRY

The study of the atmospheric degradation of some unsaturated esters

SUMMARY OF THE PHD THESIS

PhD supervisor,
Prof. univ. dr. habil. **Romeo-Iulian OLARIU**

PhD student,
Chemist **Ciprian-Paul MĂIREAN**

September 2025

Acknowledgements

Through these lines, I would like to sincerely and gratefully express my deep appreciation to those who have stood by me throughout my doctoral journey—a path that has meant both searching and growing, both scientific research and personal transformation.

I am deeply grateful to Professor Romeo-Iulian Olariu, PhD, habil., my doctoral supervisor, for the opportunity to be part of his research group, and especially for the trust, support, and generous guidance he has provided over the years. I clearly remember our first meeting, when he sincerely asked me whether I was ready to take this step, warning me that the road would not be easy. And so it was. Yet, thanks to his continuous guidance and support, I was able to overcome the challenges we faced and walk this difficult path, reaching the end with my head held high. I hope the results of our collaboration reflect our shared efforts and dedication. I am deeply grateful for everything I have learned from him, for his patience, his constructive challenges, and the example of rigor and integrity he has shown me.

I extend special thanks to the members of the guidance and academic integrity committee: Professor Cecilia Arsene, PhD, habil., Associate Professor Iustinian-Gabriel Bejan, PhD, and Professor Cezar Florin Catrinescu, PhD, habil. I thank them for their valuable advice, their support, their kind but firm expectations, and the time they devoted to my development.

I am especially thankful to the PhD. Claudiu Roman, a close colleague and mentor, for his constant support and help, for our insightful discussions, and for his personal example of commitment and professionalism that accompanied me through every stage of my research.

I would like to extend my thanks to Associate Professor Adrian Florin Șpac, PhD, who played an essential role at the beginning of this journey. At a moment of uncertainty and hesitation, he was the one who, through a simple gesture—a question asked at just the right time—managed to change the course of my professional path.

I sincerely appreciate the collegiality and wonderful collaboration within the Integrated Center for Environmental Science Studies for the North-East Development Region (CERNESIM). I thank all those who were part of this experience for their support, for the moments we shared, and for the team spirit that gave meaning to our work: PhD. Tiberiu Roman, PhD. Giorgiana

Negru, PhD. Laurențiu Șoroagă, PhD. Cornelia Niță (Amarandei), PhD students Ana-Maria Rusu (Vasilache) and Cristina Iancu.
I am profoundly grateful to PhD. Andrei Ciucă for his friendship, understanding, advice, and support, especially at the beginning of these studies.

My warmest thanks go to my family. I am deeply grateful to my wife, Cornelia, for her patience, support, and unconditional understanding throughout all these years. Her presence has been a source of strength and balance in moments of doubt and a source of joy in times of success. Emilia and Ștefan, my dear children, though perhaps too young to fully understand this journey, you have been my light and motivation. Your smiles, your hugs, and the sincere joy you bring to my life have taught me the most important lesson: that any achievement gains meaning when it is shared with loved ones. I wholeheartedly thank my mother and father for believing in me even before I fully believed in myself. I also thank my siblings for their support, encouragement, and for always being close to me, each in their own way; you never stopped being my support.

To them, I owe the beginning of this journey and the strength to see it through. Thank you all!

Acknowledgement of Financial Support

The practical activities related to this work were carried out using the infrastructure available at the CERNESIM Center of "Alexandru Ioan Cuza" University of Iași.

RECENT AIR Project, MySMIS-127324

The author acknowledges Merck Romania company for providing *Z*3HH, *Z*3H3MeB, *Z*3HBz, and *Z*3H*Z*3H free of charge.

List of research projects that financially supported the experimental part of this work:

PNIII-P2-2.1-PED2021-4119 (SOA-REACTOR)
PN-III-P4-PCE2021-0673 (ATMO-SOS)
H2020-INFRAIA-2020 - 101008004 (ATMO-ACCESS)

TABLE OF CONTENTS

INTRODUCTION

Numerous volatile organic compounds (VOCs) that are not part of the natural composition of the Earth's atmosphere are released into it (Graedel et al., 1986; Hobbs, 2000). These compounds undergo oxidation processes either near the emission source or in the upper layers of the atmosphere. The atmosphere acts as an oxidizing medium, removing these compounds through reactions with tropospheric radicals and under the influence of solar radiation (Burkholder et al., 2015). Atmospheric reactions are complex and depend on the chemical structure of the compounds, meteorological conditions, the presence of aerosols, and radiative capacity (IPCC, 2013). Although there are nighttime reactions initiated by NO_3 radicals, photochemistry remains a major driving force in atmospheric processes (Kiendler-Scharr et al., 2023). Solar radiation, depending on the wavelength, generates radicals that initiate oxidation reactions and influence atmospheric composition.

Most daily human activities result in the release of organic species into the atmosphere. Driving cars, household maintenance, cooking, spending time with friends at a barbecue, lawn care, growing plant-based animal feed, and even simple life-sustaining processes lead to significant emissions of organic compounds (VOCs) into the atmosphere (Fraser et al., 1998; Fortmann et al., 1998; Kirstine et al., 1998; Fall et al., 1999; Andreae & Merlet, 2001; Barker et al., 2006). Vegetation also releases large amounts of VOCs, especially during growth and decay processes (Finlayson-Pitts & Pitts, 2000). Emissions of biogenic volatile organic compounds exceed anthropogenic VOC emissions by an order of magnitude (Guenther et al., 2012).

Gas-phase studies require appropriate infrastructure. Atmospheric simulation chambers are essential for investigating chemical and physical processes in the atmosphere. These allow for controlled manipulation of

compounds and oxidative parameters, enabling the analysis of pollutant formation and evolution (Kiendler-Scharr et al., 2023). They provide a framework to study interactions between VOCs, solar radiation, and meteorological conditions, contributing to the identification of emission sources and the development of predictive scenarios and models.

OBJECTIVES OF THE DOCTORAL THESIS

The PhD thesis entitled "Study of the Atmospheric Degradation of Unsaturated Esters" is based on the following objectives:

i) investigation of a series of seven cis-3-hexenyl esters: formate, acetate, isobutyrate, 3-methyl butanoate, hexanoate, cis-3-hexenoate, and benzoate;

ii) determination of rate coefficients for the gas-phase reactions of cis-3-hexenyl esters with OH radicals and ozone;

iii) assessment of the atmospheric impact of the degradation of cis-3-hexenyl esters;

iv) estimation of the average atmospheric lifetimes of these esters;

v) evaluation of their potential to contribute to tropospheric ozone formation;

vi) application and evaluation of SAR (Structure–Activity Relationship) methods for estimating reaction rate constants, in comparison with experimental data;

vii) expanding the current knowledge on the atmospheric behavior of these compounds.

The doctoral thesis has the content distributed in 165 pages and includes 57 figures and 28 tables. The results presented have been published in two peer-reviewed scientific articles as first author, in journals with an impact factor of 2.7, ranked in Q2 (yellow quartile) according to the Web of Science database (Mairean et al., 2024; 2025). Some of the findings were also disseminated at four national scientific conferences

PART II: PERSONAL CONTRIBUTIONS

II.1 EXPERIMENTAL PART

I.7.1.1. ESC-Q-UAIC reactor

The atmospheric simulation chamber ESC-Q-UAIC is a cylindrical chamber with a volume of 760 ± 2 liters, composed of three quartz tubes connected by two internal flanges. It has a diameter of 0.488 meters and a total length of 4.2 meters (**Figure I.17**). The reactor is sealed at both ends with two aluminum flanges. The main (inlet) flange is equipped with a manometer for pressure monitoring and a thermocouple for measuring the temperature inside the chamber. White-type multi-reflection mirrors are mounted on the external flanges, providing an optical path length of up to 492 ± 0.2 meters in the infrared (IR) range.

Figure I.17. The ESC-Q-UAIC reaction chamber and the chamber's inlet flange.

Given that the central analytical instrument is an IR spectrometer, the water vapor level inside the chamber must be extremely low. The evacuation and cleaning of the chamber are carried out through a vacuum pump that ensures a minimum pressure of 1 × 10^-3 mbar and a flow rate of 55 m³/h. The dry air (dew point ~ -70°C) introduced into the reaction chamber comes either from a compressed air cylinder or is generated using a compressor.

The energy required for the photolysis reactions is provided by an array of 64 lamps evenly distributed around the quartz tubes: 32 Philips TL-

DK 36W superactinic lamps used for photolysis in the visible range (λ_{max} = 365 nm), and 32 Philips UV-C TUV 30W/G30 T8 germicidal lamps used for photolysis in the UV range (λ_{max} = 253.7 nm). To ensure the homogenization of the gaseous reaction mixture, two Teflon-bladed fans are used, positioned inside the reaction chamber: one on the main external flange and the other on one of the two internal flanges.

I.7.1.2. FT-IR Spectroscopy. IR Spectrometer with Extended Optical Path

The high-resolution FT-IR spectrophotometer Bruker, model Vertex 80 (**Figure I.20.**), is used for studies of simulated atmosphere. It is connected to the ESC-UAIC reactor through an optical mirror system, which directs infrared radiation into the reactor chamber, enabling real-time monitoring of gas-phase analytes. The FT-IR spectrophotometer uses infrared radiation to identify and quantify organic reactants present in the gas phase, by applying the Lambert-Beer absorption law. This technique allows precise discrimination of the analyzed compounds, contributing to a detailed understanding of the chemical processes occurring in the atmosphere.

Figure I.20. The high-resolution FT-IR spectrophotometer Bruker, model Vertex 80

The infrared radiation is generated by a silicon carbide filament, coming either from an internal MIR source or an external Globar source. The beam splitter is made of a potassium bromide (KBr) window, which is

transparent to IR radiation. Next to the spectrophotometer is a coupling box with the ESC-Q-UAIC reactor, which contains the external MCT (Mercury-Cadmium-Tellurium) detector, functioning at liquid nitrogen temperature, as well as an optical mirror system that directs the IR beam into the reaction chamber.

The IR spectra, typically obtained by composing 114 interferograms, are recorded with a spectral resolution of 1 cm^{-1} at an acquisition frequency of 60 kHz in the 700–4000 cm^{-1} range. In this configuration, the time required to acquire an IR spectrum is 60 seconds. At the beginning of each experiment, a reference spectrum (background) composed of 524 interferograms is recorded, as well as a control spectrum used to assess the presence of volatile organic compounds in the reactor.

I.7.1.3. Particle Analysis: Particle Discriminator and Counter

The Scanning Mobility Particle Sizer - Condensation Particle Counter (SMPS) (**Figure I.21.**) is a particle counter coupled with a mass classifier that helps identify the numerical distribution of formed aerosols, taking into account their mass (using a closed ionization source). This instrument is essential for monitoring the phases of secondary organic aerosol formation.

The Particle Discriminator is equipped with a TSI analyzer, capable of separating aerosols with diameters ranging from 1 to 982 nm. Inside this system, there is a metal rod through which an electric current flows, and variations in the voltage of the conductor facilitate the separation of electrostatically charged particles from the gas sample. The separation process uses a radioactive source based on 85Kr isotopes, with an initial activity of 370 MBq.

After separation, the TSI particle counter (model 3787) provides information on the number of particles in the gas system, using a light source

and an optical detector. The counter can operate in two configurations, with a sampling flow rate of 0.6 L/min and 1.5 L/min. The detectable diameter range depends on the instrument settings and its limitations.

Figure I.21. The Scanning Mobility Particle Sizer - Condensation Particle Counter (SMPS) (TSI, SUA)

The particle distributions formed in the ESC-Q-UAIC reactor are recorded online with a sampling flow rate of 0.6 L/min and a dilution flow rate of 2.7 L/min, every 110 seconds, with a 10-second pause between samples. This setting allows for the evaluation of aerosols with diameters ranging from 16.3 nm to 710.5 nm, across a concentration range of 0.2–15.0 × 10^{13} molecules cm^{-3}. Based on the particle distributions as a function of diameter and the associated numerical concentrations, the total volume and, implicitly, the total mass of the aerosols formed under the experimental conditions set for the ESC-Q-UAIC reactor can be determined.

II.1. Kinetic studies in the gas-phase in simulated atmosphere using the ESC-Q-UAIC reaction chamber

The procedure for a typical experiment involved the following steps:

1) Introduction of compounds into the reactor;
2) Homogenization of the gas mixture;
3) Determination of wall loss;

4) Determination of the photolysis rate constant;

5) Initiation of the gas-phase reaction.

II.2. Determination of the gas-phase reaction rate constant of n-butyl acetate with OH radicals

The first study conducted under controlled atmospheric conditions aimed to experimentally determine the rate constant for the reaction of n-butyl acetate (n-BuAc) with OH radicals (Măirean et al., 2020). This study aimed to validate the experimental protocol for the degradation of esters under controlled atmospheric conditions. The n-butyl acetate was chosen as a model compound due to the abundance of existing studies conducted by various research groups, which have complementary infrastructures for analyzing the reactivity of volatile organic compounds in the gas phase (Hartmann et al., 1986; Wallington et al., 1988; Williams et al., 1993; Ferrari et al., 1996; Picquet et al., 1998).

Methodologically, the relative kinetic method was used to determine the rate constant for the reaction between n-BuAc and OH radicals in the gas-phase. The experiments were carried out in the ESC-Q-UAIC chamber at a temperature of (298 ± 2) K and a pressure of (1000 ± 5) mbar, using synthetic air. The reference compounds selected for this study were acrolein, *p*-xylene, benzene, and dimethyl ether (DME). The kinetic dependencies of the gas-phase reaction of OH radicals with n-BuAc relative to the reference compounds used in this study obtained experimentally through FT-IR spectral analysis, are shown in **Figure II.3**. A comparative study of the data obtained (Table II.1) in the present study with literature data (Table II.2) highlights that the values of the rate constants for the reaction of n-butyl acetate with OH radicals are in good agreement with the values reported previously.

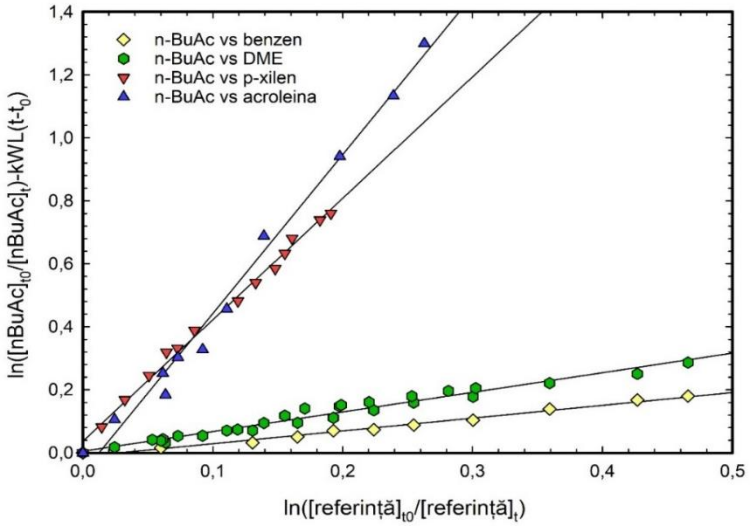

Figure II.3. Kinetic dependencies for the n-BuAc reaction with OH radicals determined relative to the references used in the current study: (▼) *p*-xylene, (◇) benzene, (▲) acrolein and (●) DME.

Table II.1: The rate constants for the reaction of n-butyl acetate with OH radicals determined under the conditions of the ESC-Q-UAIC reaction chamber (Mairean et al., 2022a).

Compound	Reference	$k_1 \times 10^{12}$ (cm^3 $molecule^{-1}$ s^{-1})	$k_{1\ (mediu)} \times 10^{12}$ (cm^3 $molecule^{-1}$ s^{-1})
n-BuAc	dimethil eter	4.51 ± 0.28	**4.03 ± 0.33**
	p-xylene	3.92 ± 0.18	
	benzene	3.96 ± 0.21	
	acrolein	3.84 ± 0.27	

II.4. Evaluation of gas-phase reaction rate constants for cis-3-Hexenyl esters with OH radicals

The evaluation of reaction rate constants for these compounds with OH radicals in the gas phase is crucial for understanding atmospheric degradation mechanisms, their persistence in the environment, and their impact on air quality and human health. The kinetic study of reactions between OH radicals and cis-3-hexenyl esters can provide valuable insights into reactivity,

intermediate products formed, and predominant reaction pathways, thus contributing to the development of predictive atmospheric models.

From an analytical perspective, the reactions between OH radicals and cis-3-hexenyl esters in the gas phase were monitored using the FT-IR technique and investigated through the relative kinetic method. This method involves using a kinetic reference compound, whose reaction constant is well-established in the literature.

The OH radicals were generated in situ by photolysis at 365 nm of methyl nitrite (CH_3ONO) or isopropyl nitrite ($(CH_3)_2CHONO$). Additionally, low NOx conditions were achieved by photolysis of hydrogen peroxide (H_2O_2) at 254 nm. Methyl nitrite was the most commonly used precursor because its photolysis has been extensively studied (Taylor et al., 1980; Atkinson et al., 1981).

The following reaction sequence outlines the gas-phase reactions that occur in the reaction chamber during the reactions between cis-3-hexenyl esters and OH radicals (Mairean et al., 2024):

ester + OH	→	products, k_{ester}
reference + OH	→	products, k_{Ref}
ester	→	products, $k_{ester,\ WL}$
reference	→	products, $k_{Ref,\ WL}$
ester + *hv* (365/254 nm)	→	products, $k_{ester,\ J}$
reference + *hv* (365/254 nm)	→	products, $k_{Ref,\ J}$

Equation II.5, derived from the integration of the kinetic equations, evaluates the ratio of reaction rate constants for the esters investigated compared to the reference compounds:

$$ln\left(\frac{[ester]_{t_0}}{[ester]_t}\right) - k_{ester,WL/J}(t - t_0) = \frac{k_{ester}}{k_{Ref}}\left(ln\ \frac{[reference]_{t_0}}{[reference]_t} - k_{Ref,WL/J}(t - t_0)\right) \quad \textbf{Eq. II.5.}$$

The individual graphical representation of $\ln([ester]_{t0}/[ester]_t) - k_{ester,WL/J}\ (t-t_0)$ as a function of $\ln([reference]_{t0}/[reference]_t)$ for each cis-3-hexenyl ester and reference compound should yield a straight line with a slope equal to k_{ester}/k_{Ref}. The reaction rate constant, k_{ester}, can be calculated using the known rate constant for the reference compound, k_{Ref}.

For each unsaturated ester, a minimum of three experiments were conducted, using at least two reference compounds to determine the rate constant. The wall loss, expressed by the wall loss constant, k_{WL}, was calculated and incorporated into the calculations to correct for the total consumption of the investigated compounds.

For the determination of the rate constants of the reactions between OH radicals and cis-3-hexenyl esters, the following reference compounds were used: isoprene, E-2-butene, cyclohexene, 1,3,5-trimethylbenzene, and propene.

Experimental data indicate that the unique exposure of cis-3-hexenyl esters and reference compounds in the gas phase to 365 nm light radiation does not result in significant additional consumption. Instead, photolysis under 254 nm radiation led to additional consumption for certain compounds. In this case, a decrease of $(11.76 \pm 1.07) \times 10^{-5}\ s^{-1}$ was observed for 1,3,5-trimethylbenzene and $(21.48 \pm 1.95) \times 10^{-5}\ s^{-1}$ for cis-3-hexenyl benzoate. For the other reference compounds, the kinetic data obtained did not show significant consumption due to photolysis, consistent with existing data in UV-Vis spectral databases (Keller-Rudek et al., 2013).

The kinetic data obtained from the investigations of OH radical reactions with cis-3-hexenyl esters, graphically represented according to Equation II.5., are presented in Figures II.7.(1-7). Table II.7. presents the experimentally obtained rate constants in this study. A linear regression analysis was performed to determine the ratio of the rate constants k_{ester}/k_{Ref}

and the associated uncertainties, expressed as 2σ confidence intervals. The absolute values of the rate constants for the ester reactions ($k_{ester,i}$) were calculated by multiplying the experimentally determined ratio by the known rate constant for the reaction of the reference compound with OH radicals ($k_{Ref,i}$). The uncertainties of the rate constant $k_{ester,i}$ were calculated using Equation II.6. by the error propagation method, considering the 2σ value obtained from the linear regression analysis and the uncertainty associated with the rate constant of the reference compound (i).

The final values of the rate constants $k_{ester+OH}$, corresponding to the reactions of unsaturated esters with OH radicals, determined under experimental conditions of high NO_x or low NO_x, were calculated using a weighted averaging method, according to Equation II.7., including the propagation of uncertainties associated with the k_{Ref} values. The value for $k_{ester,i}$ was evaluated according to Equation II.8., concerning each reference compound. The uncertainties for the $k_{(ester+OH)}$ values were estimated using Equation II.9.

The experimentally determined values for the rate constants of the reactions between OH radicals and the cis-3-hexenyl esters investigated in this study are comparable to the rate constant of the cis-3-hexene reaction, which is $(6.27 \pm 0.66) \times 10^{-11}$ cm^3 $molecule^{-1}$ s^{-1}. This similarity suggests that the dominant mechanism of the reaction between unsaturated esters and OH radicals is the addition to the double bond.

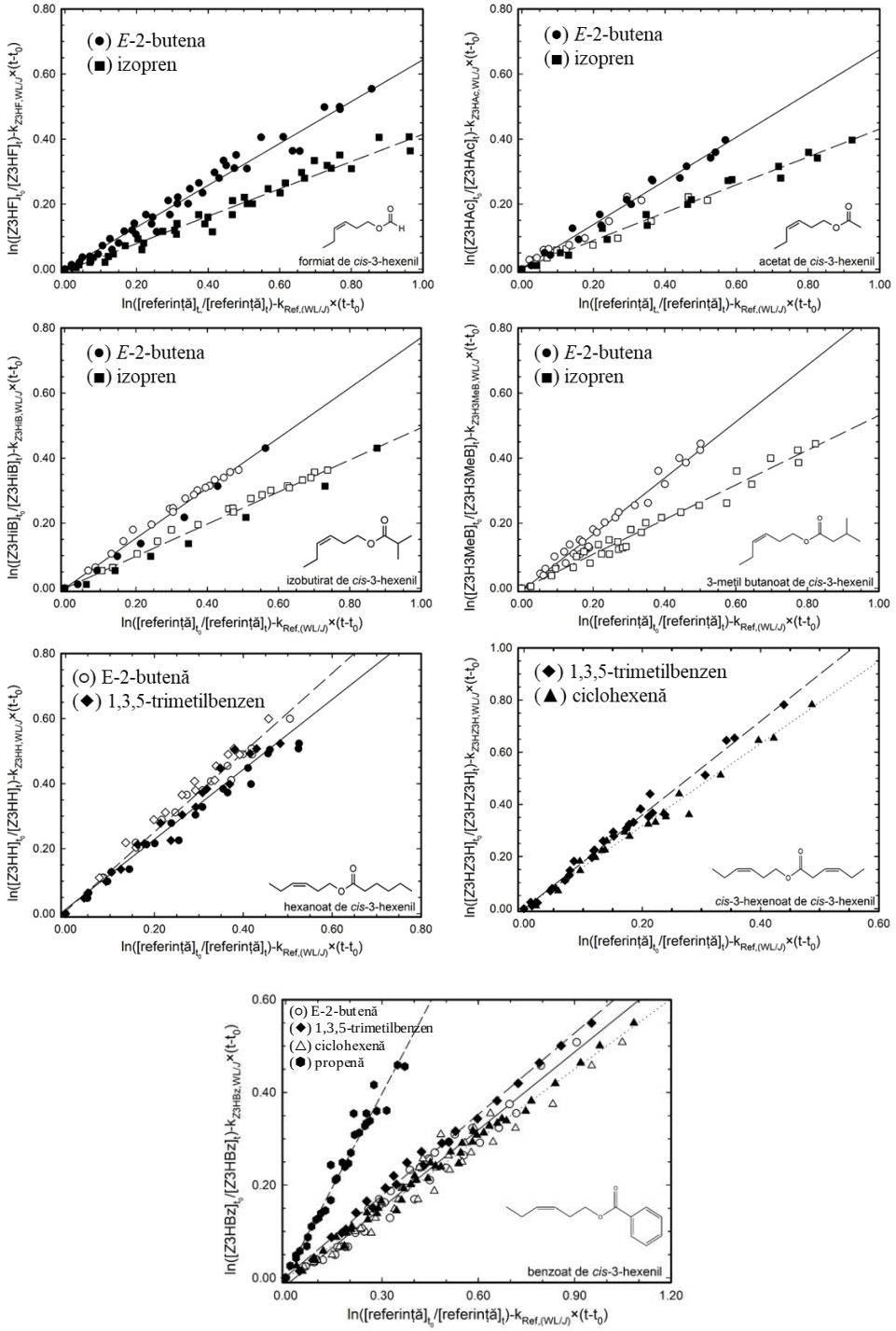

Figures II.7. (1-7). Graphical representation of the relative kinetics of cis-3-hexenyl esters with reference compounds (open symbols correspond to low NO_x conditions, and filled symbols correspond to high NOx conditions).

Table II.7: Results of the gas-phase kinetic study of the reactions of OH radicals with the investigated cis-3-hexenyl esters, using different reference compounds.

Compound	Conditions	Reference	k_{ester}/k_{ref}	$k_{ester,i} \times 10^{11}$	$k_{(ester+OH)} \times 10^{11}$	$k_{(ester+OH)(avg)} \times 10^{11}$
				(cm^3 $molecule^{-1}$ s^{-1})		
cis-3-hexenyl formate (*Z*3HF)	High NO_x	isoprene	0.42 ± 0.01	4.20 ± 0.65	4.13 ± 0.45	**4.13 ± 0.45**
		E-2-butene	0.64 ± 0.03	4.06 ± 0.63		
cis-3-hexenyl acetate (*Z*3HAc)	High NO_x	isoprene	0.43 ± 0.03	4.32 ± 0.70	4.30 ± 0.49	**4.19 ± 0,38**
		E-2-butene	0.68 ± 0.04	4.28 ± 0.69		
	Low NO_x	isoprene	0.41 ± 0.05	4.11 ± 0.81	4.04 ± 0.58	
		E-2-butene	0.63 ± 0.09	3.96 ± 0.84		
cis-3-hexenyl isobutyrate (*Z*3HiB)	High NO_x	isoprene	0.48 ± 0.04	4.78 ± 0.82	4.79 ± 0.57	**4.84 ± 0.39**
		E-2-butene	0.76 ± 0.05	4.81 ± 0.79		
	Low NO_x	isoprene	0.50 ± 0.45	4.96 ± 0.77	4.88 ± 0.53	
		E-2-butene	0.76 ± 0.03	4.81 ± 0.75		
cis-3-hexenyl 3 methylbutanoate (*Z*3H3MeB)	Low NO_x	isoprene	0.53 ± 0.03	5.31 ± 0.84	5.39 ± 0.61	**5.39 ± 0.61**
		E-2-butene	0.87 ± 0.05	5.47 ± 0.87		
cis-3-hexenyl hexanoate (*Z*3HH)	High NO_x	1,3,5-trimethylbenzene	1.17 ± 0.08	6.84 ± 1.12	6.60 ± 0.76	**7.00 ± 0.56**
		E-2-butene	1.02 ± 0.05	6.41 ± 1.02		
	Low NO_x	1,3,5-trimethylbenzene	1.29 ± 0.06	7.54 ± 1.19	7.48 ± 0.84	
		E-2-butene	1.17 ± 0.06	7.41 ± 1.17		
cis-3-hexenyl *cis*-3-hexenoate (*Z*3HZ3H)	High NO_x	1,3,5-trimethylbenzene	1.80 ± 0.07	10.54 ± 1.64	10.58 ± 1.40	**10.58 ± 1.40**
		ciclohexene	1.58 ± 0.07	10.68 ± 2.72		
cis-3-hexenyl benzoate (*Z*3HBz)	High NO_x	1,3,5-trimethylbenzene	0.58 ± 0.02	3.43 ± 0.52	3.33 ± 0.34	**3.41 ± 0.28**
		ciclohexene	0.51 ± 0.01	3.43 ± 0.86		
		propene	1.31 ± 0.08	3.20 ± 0.52		
	Low NO_x	ciclohexene	0.49 ± 0.03	3.33 ± 0.85	3.57 ± 0.47	
		E-2-butene	0.58 ± 0.02	3.67 ± 0.57		

The experimental values obtained allowed the establishment of the following reactivity trend, also illustrated in Figure II.10 (Mairean et al., 2024): *cis*-3-hexenyl benzoate < cis-3-hexenyl formate ≈ cis-3-hexenyl acetate < cis-3-hexenyl isobutyrate < cis-3-hexenyl 3-methylbutanoate < cis-3-hexenyl hexanoate << cis-3-hexenyl cis-3-hexenoate.

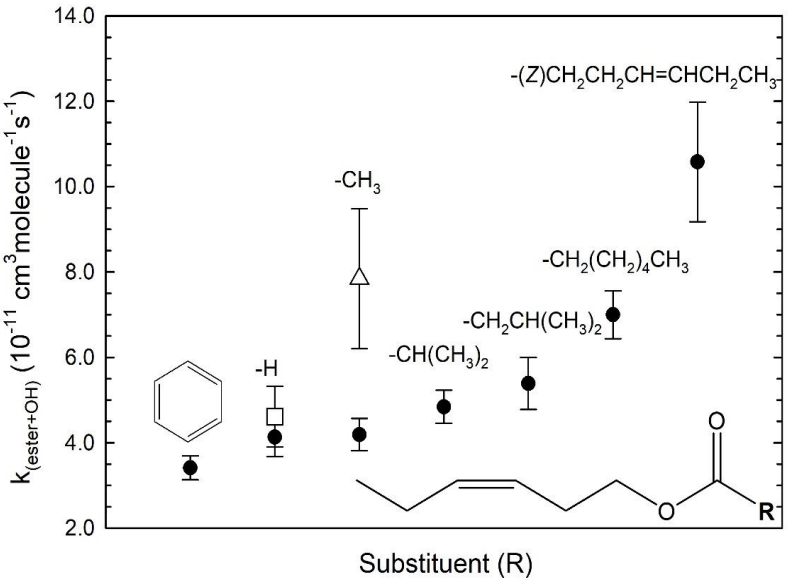

Figure II.10. Graphical representation of the reactivity trend of the (circle solid) investigated unsaturated esters with OH radicals in the gas-phase at the temperature of (298 ± 2) K and pressure of (1000 ± 10) mbar. Data from Atkinson et al., 1995 (△) și Rodríguez et al., 2015 (□) studies.

The variation in OH reactivity for the saturated esters within this series is influenced by the increase in the carbon chain length, resulting in multiple sites for hydrogen atom abstraction from the molecules. The low reactivity of cis-3-hexenyl benzoate in this series can be explained by the electron-withdrawing electromeric effect exerted by the ester group on the aromatic ring. This phenomenon, characteristic of type II aromatic substituents, significantly reduces reactivity toward OH radicals, similar to other deactivated aromatic compounds (e.g., nitrophenols or nitrocatechols, as

reported by Bejan et al., 2007; Roman et al., 2022). In this context, the OH reactivity of the benzoate becomes comparable to that of nitrobenzene ((1.40 ± 0.49) × 10^{-13} cm^3 $molecule^{-1}$ s^{-1} (Witte et al., 1986; Calvert et al., 2002), indicating a negligible contribution to the overall observed reactivity. The inductive effect alone cannot adequately explain the differences in reactivity toward OH radicals between these compounds, as it decreases exponentially in intensity with each additional carbon atom moving away from the functional group.

Comparing cis-3-hexenyl isobutyrate and 3-methylbutanoate, an increase in the reaction rate constant of approximately 0.5 × 10^{-11} cm^3 $molecule^{-1}$ s^{-1} was observed for each added secondary carbon atom (-CH_2-). Therefore, considering the reactivity of cis-3-hexenyl acetate, (4.2 ± 0.5) × 10^{-11} cm^3 $molecule^{-1}$ s^{-1}, it can be estimated that the rate constant for cis-3-hexenyl hexanoate should be around 6.2 × 10^{-11} cm^3 $molecule^{-1}$ s^{-1}, a value close to that determined experimentally.

The addition of a tertiary carbon atom (>CH–) in the case of isobutyrate relative to cis-3-hexenyl acetate contributed to an increase in reactivity of approximately 0.6 × 10^{-11} cm^3 $molecule^{-1}$ s^{-1}. No significant effect was observed for the –CH_3 group when comparing the reactivity of cis-3-hexenyl formate to that of cis-3-hexenyl acetate. The analysis of the difference between hexanoate and cis-3-hexenyl cis-3- hexenoate allows the estimation of the contribution of the second double bond to the total reactivity, evaluated at approximately 3.0 × 10^{-11} cm^3 $molecule^{-1}$ s^{-1}. According to hypotheses derived from experimental rate coefficient values, the estimated rate constants for the gas-phase reactions with OH radicals for cis-3-hexenyl pentanoate and methyl-pentanoate are approximately 5.7 × 10^{-11} cm^3 $molecule^{-1}$ s^{-1} and 5.8 × 10^{-11} cm^3 $molecule^{-1}$ s^{-1}, respectively. Comparison of the present results with literature data (Ren et al., 2019; Sun et al., 2016) highlights similar trends in

OH reactivity for methacrylates and cis-3-hexenyl esters. An average difference of approximately 0.5 × 10^{-11} cm^3 $molecule^{-1}$ s^{-1} was observed in comparative studies of esters with successive carbon chains, emphasizing the consistency of this trend in similar series.

The significant difference between cis-3-hexenol and hexanol (~ 9.5 × 10^{-11} cm^3 $molecule^{-1}$ s^{-1}) reflects the major contribution of OH radical addition to the double bond, leading to β-hydroxy radical formation, a mechanism also confirmed by theoretical studies (Sun et al., 2016).

II.4.2. Estimation of the reactivity of cis-3-hexenyl esters with OH radicals based on Structure–Activity Relationship (SAR) models

In this study, the rate constants for gas-phase reactions of cis-3-hexenyl esters with OH radicals were estimated using four SAR approaches: the model proposed by Kwok and Atkinson (1995), the EPI Suite AOPWIN program developed by the United States Environmental Protection Agency (based on the algorithm and factors proposed by Kwok and Atkinson), the polyalkene model proposed by Peeters et al. (2007), and the model proposed by Jenkin et al. (2018a), later extended by Jenkin et al. (2018b).

Table II.9 presents the rate constants calculated according to the SAR methods mentioned above for the series of unsaturated esters considered in this study. **Tables II.10–II.13** detail the procedure for calculating the k_{SAR} for each cis-3-hexenyl ester using the corresponding methodologies. This contribution was added to the total estimated value for the aliphatic branch, in accordance with the corresponding SAR methodology. The contribution is minor, representing less than 2% of the total rate constant at 298 K (Mairean et al., 2024).

The analysis of the contribution of the hydrogen atom abstraction channel by OH radicals, according to the SAR methods used, reveals that it

accounts for approximately 21% of the overall reactivity according to the methodology of Jenkin et al. (2018a; 2018b) and about 9% according to the Kwok and Atkinson (1995) method. In general, the Jenkin et al. method offers more accurate estimates for esters with longer carbon chains, as it explicitly accounts for the effect of substituents on the overall reactivity of the compounds. A comparison of estimates shows that for molecules with longer carbon chains, the SAR methodology proposed by Jenkin et al. (2018a; 2018b) is more accurate than the one proposed by Kwok and Atkinson (1995).

A visual representation of the correlation between the SAR-estimated values and those obtained in the current study is provided in **Figure II.11**.

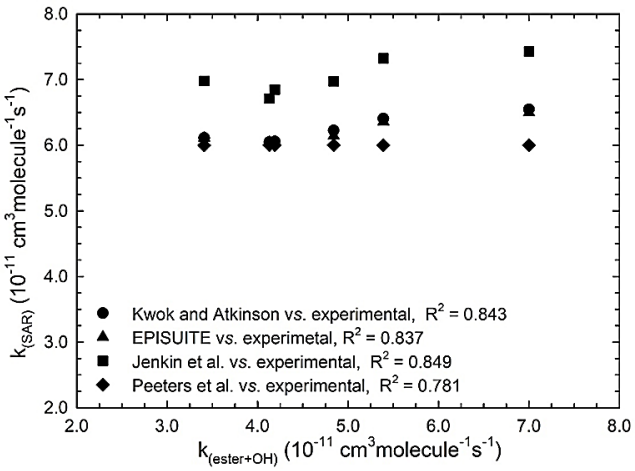

Figure II.11. Correlation between the SAR estimates and the experimentally determined gas-phase OH-initiated reaction rate coefficients of the investigated Z3HF, Z3HAc, Z3HiB, Z3H3MeB, Z3HH, and Z3HBz.

Table II.9: Experimental and SAR-estimated rate coefficients of cis-3-hexenyl ester compounds with the OH radicals. The ratios of the estimated values to the experimental data (k_{SAR}/k_{exp}) are given in brackets.

Compound	$k_{(ester+OH)} \times 10^{11}$ (cm^3 $molecule^{-1}$ s^{-1})					
	Mairean et al., 2024	Literature	k_{SAR}			
			EPI Suite-AOPWIN[a]	Kwok and Atkinson (1995)	Jenkin et al. (2018a,b)	Peeters et al. (2007)
Z3HF	4.13 ± 0.45	4.61 ± 0.71[b]	6.05 (1.46)	6.05 (1.46)	6.71 (1.63)	6.00 (1.45)
Z3HAc	4.19 ± 0.38	7.74 ± 1.50[c]	6.05 (1.44)	6.05 (1.45)	6.85 (1.63)	6.00 (1.43)
Z3HiB	4.84 ± 0.39		6.14 (1.27)	6.23 (1.29)	6.97 (1.44)	6.00 (1.24)
Z3H3MeB	5.39 ± 0.61		6.36 (1.18)	6.41 (1.19)	7.32 (1.36)	6.00 (1.11)
Z3HH	7.00 ± 0.56		6.50 (0.93)	6.55 (0.94)	7.43 (1.06)	6.00 (0.86)
Z3HZ3H	10.58 ± 1.40		11.83 (1.12)	11.87 (1.12)	13.01 (1.23)	12.00 (1.13)
Z3HBz	3.41 ± 0.28		6.11 (1.79)	6.11 (1.79)	6.98 (2.05)	6.00 (1.76)

[a] US EPA; [b] Rodriguez et al., (2015); [c] Calvert et al., (2015).

II.4.3. Evaluation of secondary organic aerosol (SOA) formation from OH radical oxidation of unsaturated esters in simulated atmosphere

The study investigated the formation of secondary organic aerosols (SOAs) resulting from the gas-phase photo-oxidation of cis-3-hexenyl esters by OH radicals under simulated atmospheric conditions. Experiments were conducted under both low-NO_x and high-NO_x concentration conditions. The reactions were performed using initial concentrations of approximately 5×10^{13} molecules cm^{-3} for the esters under study. No OH radical scavenger was used, and the relative humidity was approximately 2%. The consumption of unsaturated esters during the experiments was monitored using FT-IR spectroscopy, while the formation and evolution of secondary organic aerosols were measured using a tandem system composed of a particle counter coupled with a particle size and volume classifier.

For the low-NO_x experiment, the OH radicals were generated via the photolysis of H_2O_2 at 254 nm in the atmospheric simulation chamber. In experiments carried out under high-NO_x conditions, OH radicals were generated by photolysis of isopropyl nitrite at 365 nm.

II.4.3.1. *cis*-3-hexenyl acetate + OH (Low-NO_x)

Secondary Organic Aerosols were generated through the gas-phase photo-oxidation of cis-3-hexenyl acetate using the 32 germicidal lamps (λ_{max} = 254 nm) of the ESC-Q-UAIC chamber. H_2O_2 was introduced into the reactor in a measured volume. Preliminary tests indicated that cis-3-hexenyl acetate does not undergo photolysis under the conditions of the ESC-Q-UAIC chamber, and the observed loss during exposure to 254 nm radiation was attributed exclusively to wall deposition within the reactor. This physical loss was experimentally quantified and included in the corrections applied during subsequent kinetic determinations.

After introducing and monitoring the compounds for several minutes, the germicidal lamps (λ_{max} = 254 nm) were switched on, generating OH radicals via photolysis of the previously introduced precursor (H_2O_2). The concentration of the unsaturated ester and the formation of secondary organic aerosols were continuously monitored using FT-IR spectroscopy (Bruker Vertex 80) and a tandem analytical system composed of a differential mobility analyzer and a particle counter (TSI SMPS-CPC).

Figure II.13 shows the particle mass concentration distribution as a function of diameter during the photo-oxidation reaction of cis-3-hexenyl acetate by OH radicals under low-NOx conditions. The mass concentration distribution indicates the formation of aerosols with small diameters during photolysis at 254 nm, but the mass concentration of these particles is insignificant.

Figure II.14 illustrates the oxidation process of cis-3-hexenyl acetate resulting from its reaction with OH radicals under low-NO_x conditions. Once the lamps are turned on and OH radicals are generated, cis-3-hexenyl acetate is rapidly consumed (the graph highlights the duration of the reaction), followed by the formation of new particles and instantaneous nucleation. The particle mass concentration and number increase accordingly. This behavior is typical of atmospheric oxidation processes, where primary pollutants are transformed into secondary particles that contribute to air pollution and can impact health and climate. The number concentration of SOAs peaked within about 10 minutes and then decreased significantly, most likely due to the partitioning of these small particles into and/or with the gas-phase products.

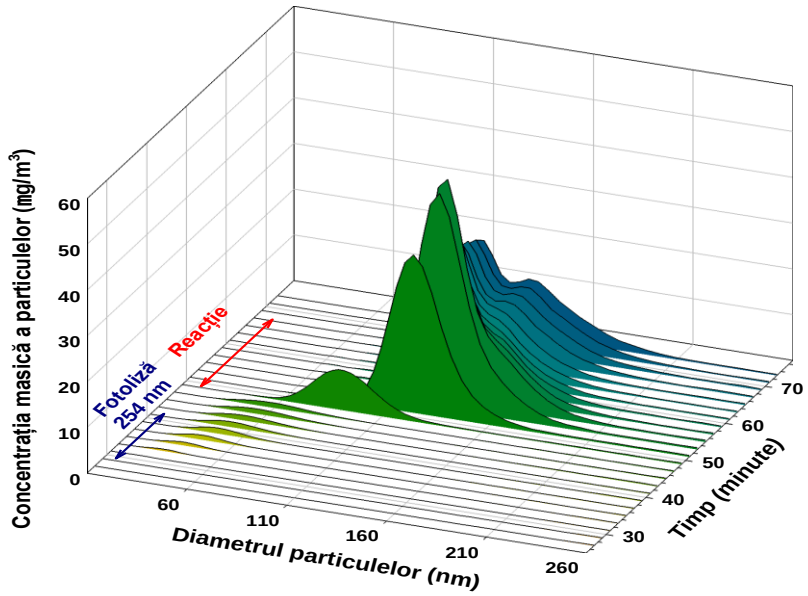

Figure II.13. Mass distribution of SOAs formed from the reaction of cis-3-hexenyl acetate with OH radicals under the conditions of the ESC-Q-UAIC chamber, at 298 K, 1000 mbar air, and low NO_x conditions.

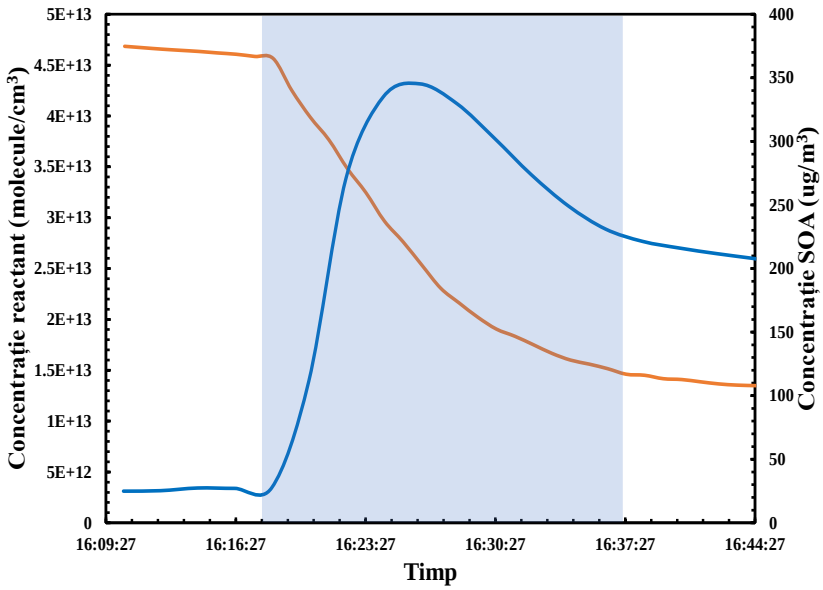

Figure II.14. Formation of SOAs from the photo-oxidation of cis-3-hexenyl acetate by OH radicals under the conditions of the ESC-Q-UAIC chamber, at 298 K and 1000 mbar air, under low NO_x conditions.

The size and number distribution of aerosols indicate a correlation between chemical processes (oxidation and nucleation) and physical processes (growth and coagulation) in the formation of SOAs. Low-NO_x conditions favor SOA formation through radical-driven mechanisms involving the direct oxidation of the ester, significantly affecting both particle size and number.

II.4.3.2. *cis*-3-hexenyl acetate+ OH (High NO_x)

The signal distribution recorded following the reaction of cis-3-hexenyl acetate with OH radicals under high NO_x conditions in the reaction chamber is presented in Figure II.19. No SOA formation was observed or measured as a result of this reaction.

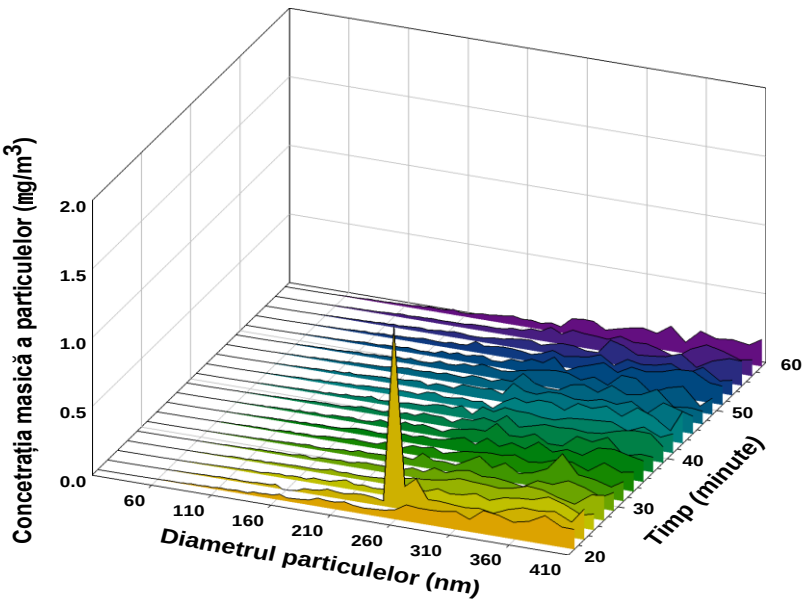

Figure II.19. The signal distribution recorded following the reaction of cis-3-hexenyl acetate with OH radicals under the conditions of the ESC-Q-UAIC chamber, at 298 K, 1000 mbar air pressure, and high NO_x conditions.

Under high NO_x conditions, no secondary organic aerosols are formed following the reaction between cis-3-hexenyl acetate and OH radicals. Most likely, the aerosol formation process is hindered by the experimental high NO_x

conditions, which suppress the formation of intermediate radicals responsible for generating aerosol precursors.

II.5. Kinetic studies for evaluating the gas-phase ozonolysis rate constants of cis-3-hexenyl esters

Although reactions with OH radicals are considered the main mode of removal for cis-3-hexenyl esters from the atmosphere, reactions with ozone may become increasingly important, especially in urban areas with high NO_x levels. In these areas, high NO_x levels can suppress OH radical formation through reaction with them, forming nitric acid (HNO_3). This reduction in OH radical concentration increases the relative importance of the ozone reaction pathway for volatile organic compounds (Mollner et al., 2010).

II.5.1. Determination of kinetic rate constants for gas-phase reactions of cis-3-hexenyl esters with ozone

This study presents experimental results regarding the gas-phase ozonolysis of a series of seven cis-3-hexenyl unsaturated esters and provides new kinetic data that expand the existing databases and SAR methodologies applied to ozonolysis reactions. Currently, no kinetic measurements have been reported for the reactions of ozone with cis-3-hexenyl isobutyrate, cis-3-hexenyl 3-methylbutanoate, cis-3-hexenyl hexanoate, cis-3-hexenyl cis-3-hexenoate, or cis-3-hexenyl benzoate.

To assess the reaction rate coefficients for the gas-phase ozonolysis of a series of cis-3-hexenyl esters, a series of investigations were conducted at a temperature of 298 K and an air pressure of 1 atm. The experiments were carried out using the atmospheric simulation chamber at the "Alexandru Ioan Cuza" University of Iași (ESC-Q-UAIC), Romania. The relative kinetic method was used to experimentally determine the rate coefficients for the gas-

phase ozonolysis of selected cis-3-hexenyl esters. Rate constants for the reactions of ozone with cis-3-hexenyl esters were determined by comparing the consumption rates with those for the following reference compounds: cyclohexene, *E*-2-butene, and propene.

Experimental conditions for ozonolysis reactions

Ozone was generated by passing a constant flow of oxygen over a mercury lamp emitting at a wavelength of 184.9 nm, which was subsequently directed into the reactor to initiate the oxidation. Weighed quantities of 1,3,5-trimethylbenzene (TMB) were added to the reactor in each experiment as a tracer species, allowing the evaluation of the OH radicals produced. Continuous monitoring of TMB in the reactor allowed for corrections to be made for the degradation of cis-3-hexenyl esters and reference compounds, caused by the interference of secondary reactions initiated by OH radicals generated during the ozonolysis of unsaturated volatile compounds. For each compound, loss through adsorption on the reactor walls (expressed by the wall loss constant, k_{WL}) was evaluated, and where necessary, appropriate corrections were applied to the final kinetic equation.

The following reaction sequence presents the processes occurring during the gas-phase interactions of cis-3-hexenyl esters with O_3 at (298 ± 2) K and a total air pressure of (1000 ± 10) mbar:

ester + O_3	→	products (+ HO)·	k_{ester}
reference + O_3	→	products (+ HO·)	k_{ref}
ester	→	Wall reactor	$k_{ester, WL}$

Equation II.11, derived from the integration of the kinetic equations, allows for the evaluation of the ratio of the reaction rate constants for the investigated esters relative to the reference compounds:

$$ln\left(\frac{[ester]_{t_0}}{[ester]_t}\right) - k_{ester,WL} \times (t - t_0) = \frac{k_{ester}}{k_{ref}}\left(ln\left(\frac{[\text{reference}]_{t_0}}{[\text{reference}]_t}\right)\right) \quad \textbf{Eq. II.11.}$$

where: $[ester]_{t0}$ and $[reference]_{t0}$ represent the initial concentrations of the cis-3-hexenyl esters and the reference compounds at the initial time. t_o; $[ester]_t$ and $[reference]_t$ are the concentrations of the cis-3-hexenyl esters and the reference compounds at a given time, *t*, during the reaction.

Graphical representation of the relationship. $ln([ester]_{t0}/[ester]_t) - k_{ester,WL}\ (t-t_0)$ as a function of $ln([reference]_{t0}/[reference]_t)$ for each cis-3-hexenyl ester and reference compound, the plot should yield a straight line with a slope equal to k_{ester} / k_{ref}. The reaction rate constant, k_{ester}, can be determined using the known reaction rate constant of the reference compound, k_{ref}.

The use of a tracer compound instead of an OH radical scavenger allows for the correction of additional analyte conversion caused by OH-initiated reactions during ozonolysis. In this study, 1,3,5-trimethylbenzene was used as a tracer compound because it does not react with ozone molecules, reacts exclusively with OH radicals (Paulson et al., 1999; Rickard et al., 1999), and exhibits distinct IR spectral features, facilitating spectral analysis.

In addition to the initial reactions in the gas mixture, the following reactions also occur when a tracer compound is used:

ester + OH	→	products	k'_{ester}
reference + OH	→	products	k'_{ref}
tracer+ OH	→	products	k'_{tracer}
tracer	→	Wall reactor	$k'_{tracer,WL}$

Following the consumption mechanism of the tracer compound, the concentration of OH radicals can be determined using Equation II.12. This allows for the quantification of the impact of OH radicals on the reaction kinetics within the gas mixture and the correction of additional losses of cis-

3-hexenyl esters and reference compounds. As a result, it ensures a rigorous analysis of atmospheric ozonolysis processes.

$$[OH] = \left(\ln\left(\frac{[T]_{t_0}}{[T]_t}\right) - k'_{tracer,WL} \times (t - t_0\right) \times \frac{1}{k'_{tracer} \times (t - t_0} \quad \textbf{Eq. II.12.}$$

where:

- ✓ $[T]_{to}$ and $[T]_t$ represents the concentrations of the tracer compound at the initial time t_0 and reaction time t;
- ✓ $k'_{tracer,WL}$ is the wall loss rate constant of the tracer compound in the reactor;
- ✓ k'_{tracer} is the gas-phase rate constant of the reaction between OH radicals and the tracer compound, determined under the experimental temperature and pressure conditions.

Equation Eq. II.13 takes into account the secondary chemical reactions initiated by OH radicals in the gas mixture and is derived from Equation Eq. II.11. It allows for the correction of additional losses of cis-3-hexenyl esters and reference compounds, providing a more accurate assessment of the ozonolysis kinetics under simulated atmospheric conditions:

$$ln\left(\frac{[ester]_{t_0}}{[ester]_t}\right) - (k_{ester,WL} + k'_{ester} \times [OH]) \times (t - t_0) = \frac{k_{ester}}{k_{reference}}\left(ln\left(\frac{[reference]_{t_0}}{[reference]_t}\right) - k'_{reference} \times [OH] \times (t - t_0)\right) \quad \textbf{Eq. II.13.}$$

This approach allows for the determination of reaction rate coefficients for the ozonolysis of cis-3-hexenyl esters, correcting for losses caused by secondary reactions initiated by OH radicals. The slope value in the graphical

representation mentioned above provides the ratio of the reaction rate coefficients for the ozonolysis of the studied compounds compared to the reference compounds.

Table II.15: Results of the gas-phase kinetic study of the reactions of O_3 molecules with the investigated *cis*-3-hexenyl esters.

Compound	Reference	k_{ester}/k_{ref}	$k_{ester,i} \times 10^{17}$	$k_{(ester+O3)(avg)} \times 10^{17}$
			(cm^3 $molecule^{-1}$ s^{-1})	
cis-3-hexenyl formate	propene	4.09 ± 0.19	4.21 ± 0.19	**4.53 ± 0.50**
	ciclohexene	0.60 ± 0.02	4.94 ± 0.13	
cis-3-hexenyl acetate	propene	4.77 ± 0.16	4.91 ± 0.16	**5.51 ± 0.60**
	ciclohexene	0.80 ± 0.01	6.54 ± 0.11	
cis-3-hexenyl isobutyrate	propene	7.26 ± 0.23	7.48 ± 0.24	**7.89 ± 0.85**
	ciclohexene	1.04 ± 0.03	8.40 ± 0.25	
cis-3-hexenyl 3-methylbutanoate	*E*-2-Butene	0.57 ± 0.02	11.50 ± 0.40	**11.94 ± 1.30**
	ciclohexene	1.54 ± 0.05	12.50 ± 0.40	
cis-3-hexenyl hexanoate	*E*-2-Butene	0.76 ± 0.04	15.20 ± 0.83	**15.34 ± 1.74**
	ciclohexene	1.91 ± 0.11	15.50 ± 0.90	
cis-3-hexenyl *cis*-3-hexenoate	*E*-2-Butene	1.02 ± 0.04	20.40 ± 0.88	**22.45 ± 2.53**
	ciclohexene	3.21 ± 0.18	26.00 ± 1.48	
cis-3-hexenyl benzoate	*E*-2-Butene	1.40 ± 0.03	28.00 ± 0.68	**29.11 ± 3.20**
	ciclohexene	3.73 ± 0.20	30.40 ± 1.64	

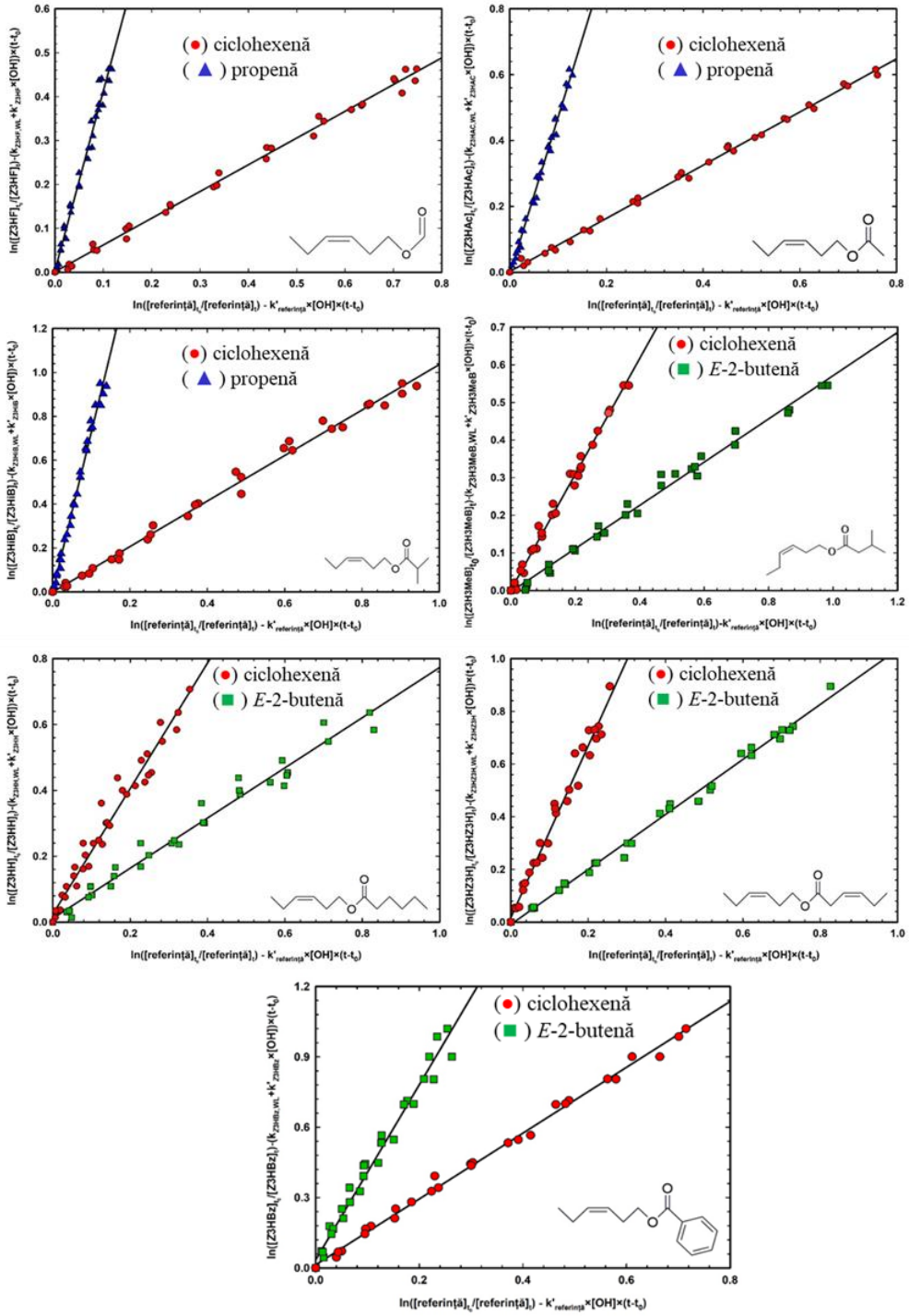

Figure II.20.1-7. Relative kinetic plots of the ozone reaction with *cis*-3-hexenyl esters versus reference compounds (Mairean et al., 2025)

To evaluate the contribution of each reaction mechanism (with ozone, OH radicals, and wall losses) to the conversion of cis-3-hexenyl esters and reference compounds, Figure II.22 presents the relative fractions consumed by these processes during the kinetic experiments. All conversion values of the analytes (expressed as percentages relative to the signal obtained before the initiation of ozonolysis), including those for reference and tracking compounds, influenced by wall losses as well as reactions initiated by ozone and OH, are presented in Figure II.22 and Table II.16 (Mairean et al., 2025).

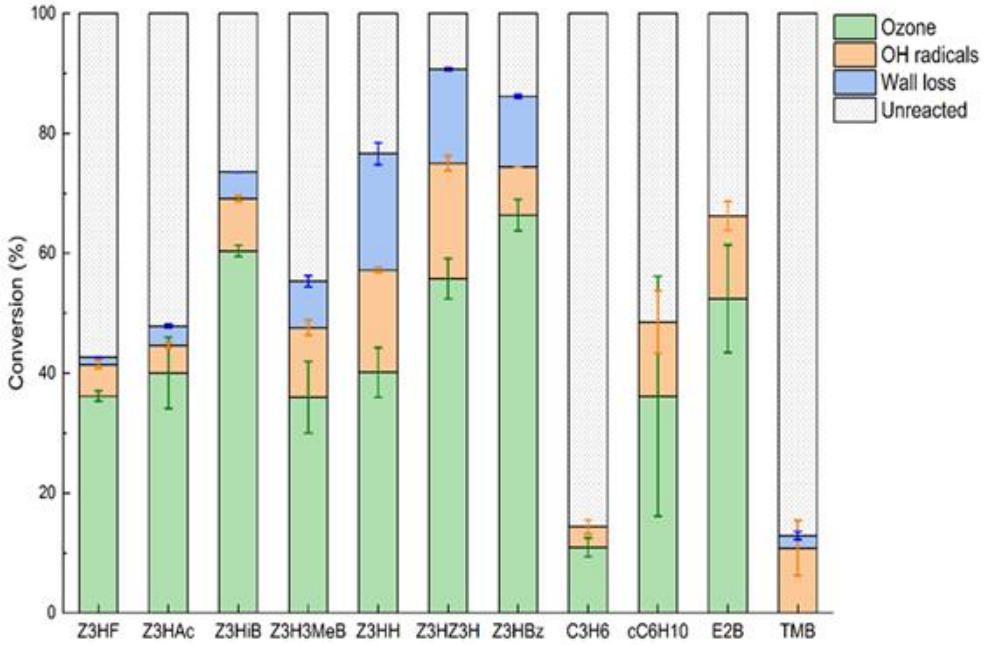

Figure II.22. The conversions of cis-3-hexenyl esters, the reference and the tracer compounds during the kinetic measurements due to wall losses, OH, and ozone gas-phase reactions.

II.5.2. Variation in gas-phase reactivity of cis-3-hexenyl ester reactions with ozone

The experimental results presented suggest that reactivity towards ozone is influenced both by the size of the acyl group and the degree of unsaturation of

the compound. The variation in the reaction rate coefficients for unsaturated esters follows a clear trend, as indicated by the series:

*Z*3HF < *Z*3HAc < *Z*3HiB < *Z*3H3MeB < Z3HH < *Z*3HZ3H < *Z*3HBz.

The hierarchical arrangement suggests that as the acyl group becomes larger or more unsaturated, reactivity towards ozone increases, likely due to the enhanced electron density and structural factors associated with these changes. This trend can also be attributed to the increased conjugation of the electronic systems within the unsaturated esters, which enhances their susceptibility to ozone addition, as observed in derivatives with higher degrees of unsaturation and larger acyl groups, such as Z3HBz.

Figure II.23 provides a visual representation of this trend and allows a comparative analysis with existing literature, including compounds such as Z3HF, Z3HAc, cis-3-hexene, cis-3-hexen-1-ol, and cis-3-hexenal. The insert presents the linear distribution of the log-transformed weighted values of the reaction rate coefficients for the ozonolysis of cis-3-hexenyl esters with saturated acyl fragments, based on the number of carbon atoms, highlighting the importance of the inductive electronic effect of the R group on the overall inductive effect of the ester functional group concerning the double bond. The comparisons made contribute to the contextualization of the reactivity patterns observed concerning the existing data in the literature, thus providing a broader understanding of how molecular structure influences the reactivity of unsaturated esters towards ozone.

The experimental data indicate that the gas-phase reaction rate coefficients of cis-3-hexenyl esters (formate, acetate, and isobutyrate) with ozone molecules are lower compared to that of cis-3-hexene, which has a reaction coefficient of $(1.44 \pm 0.43) \times 10^{-16}$ cm^3 molecule^{-1} s^{-1} (Calvert et al., 2015). In contrast, the reaction rate coefficients for cis-3-hexenoate and cis-3-hexenyl benzoate are higher, while those for 3-methylbuthanoate and

hexanoate of cis-3-hexenyl are similar to the reference value (Mairean et al., 2025).

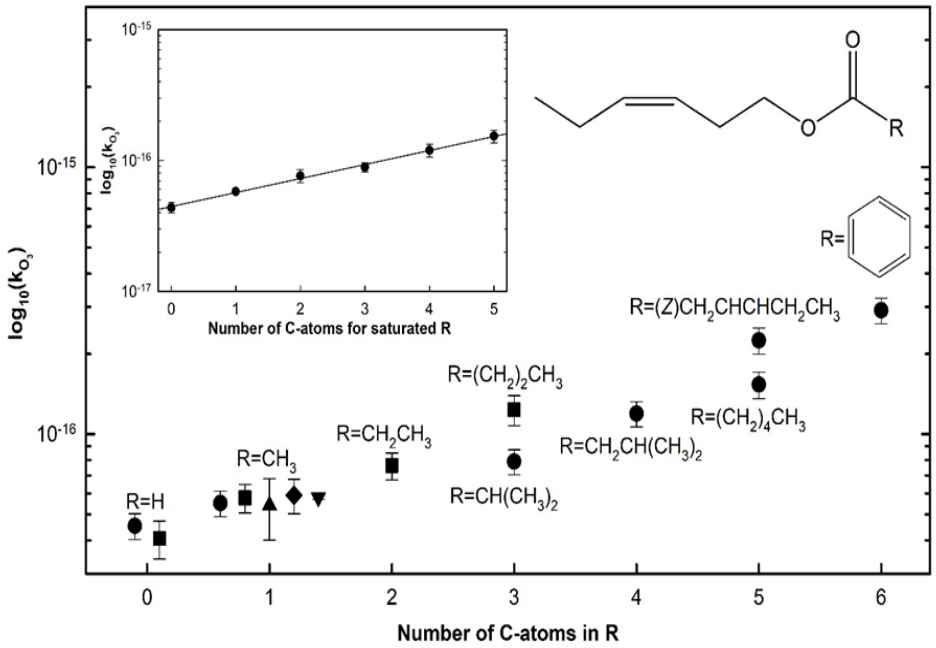

Figure II.23. Graphical representation of the gas-phase reactivity trend for the ozonolysis of *cis*-3-hexenyl esters at a temperature of (298 ± 2) K and atmospheric air pressure. Data from (●) Mairean et al., 2025, (■) Zhang et al. (2018), (▲) Atkinson et al. (1995), (◆) Grosjean și Grosjean (1998) and (▼) Harvey et al. (2015). The inset figure shows the linear distribution of the logarithm of the weighted ozonolysis rate coefficients, compiled from all available literature studies, including the present work, for *cis*-3-hexenyl esters containing saturated acyl moieties, plotted against the number of C atoms.

The ozonolysis rate coefficients of cis-3-hexenyl esters are at least equal to or greater than those of cis-3-hexenol ((4.13 ± 0.34) × 10^{-17} cm^3 $molecule^{-1}$ s^{-1}; Grira et al., 2022) and cis-3-hexenal ((3.50 ± 0.20) × 10^{-17} cm^3 $molecule^{-1}$ s^{-1}; Xing et al., 2012). This observation is explained by the reduced electron-withdrawing inductive effect exerted by the ester group, due to the electron-donating inductive effect of the acyl groups, supporting the hypothesis put forward by Zhang et al. (2018). Kinetic studies on

methacrylates have demonstrated the influence of the acyl and alkoxyl group structures on ozone reactivity (Ren et al., 2019).

The analysis of the data presented in Table II.17 shows a positive correlation between the reaction rate coefficient (k) and the length of the alkoxyl group, as previously reported for a series of vinyl ethers (Al Mulla et al., 2010; Zhou et al., 2012; Colmenar et al., 2015). In the case of cis-3-hexenyl benzoate, the aromatic ring acts as an electron donor through conjugative effects, compensating for the electron-withdrawing inductive effect of the ester group, as illustrated in Figure II.24.

Regarding reactivity towards OH radicals, the presence of the aromatic ring does not significantly affect reactivity, as the aromatic sites are negligible (Mairean et al., 2024). The existence of cis/trans conformation, suggested by Zhang et al. (2018), indicates that the trans form is energetically more stable, and the aromatic planar geometry may reduce steric effects compared to similar aliphatic esters.

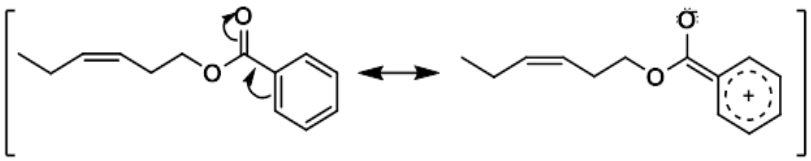

Figure II.24. Electromeric effect occurring within the *cis*-3-hexenyl benzoate molecule, leading to a significant increase in the reactivity toward ozone by opposing the electron-withdrawing effect of the ester functional group.

II.5.3. Estimation of cis-3-hexenyl ester reactivity with ozone according to SAR models

In the absence of direct experimental measurements, SAR methods serve as a valuable tool for estimating reaction rate constants for these reactions and for characterizing the mechanisms involved (Mairean et al., 2025).

In the present study, four SAR methods (Atkinson and Carter, 1984; McGillen et al., 2008, 2011; Calvert et al., 2002; Jenkin et al., 2020) were used

to estimate the values of gas-phase reaction rate constants for a series of cis-3-hexenyl esters with O_3. These methods were developed based on extensive experimental data sets and can provide a reasonable estimate of the reactivity of unsaturated compounds towards ozone.

The experimentally obtained rate constants for the ozonolysis of cis-3-hexenyl esters were compared with the rate constants calculated using different SAR approaches. The comparative analysis between experimental data and SAR estimates highlights the limitations of current methodologies in accurately estimating the reaction rate coefficients for the reaction between ozone and cis-3-hexenyl esters.

Table : Experimental and SAR-estimated reaction rate constants for cis-3-hexenyl esters with ozone. The ratios between the estimated values and experimental data (k_{SAR}/k_{exp}) are given in brackets.

Compound	$k_{(ester+O3)} \times 10^{17}$ (cm^3 molecule^{-1} s^{-1})					
			SAR (k_{SAR}/k_{exp})			
	Mairean et al., 2025	Zhang et al., 2018	Atkinson and Carter, 1984	Calvert et al., 2000	McGillen et al., 2011	Jenkin et al., 2020
cis-3-hexenyl formate	**4.53 ± 0.50**	4.06 ± 0.66	**13** (2.89)	**12** (2.67)	**3.6** (0.79)	**12** (2.67)
cis-3-hexenyl acetate	**5.51 ± 0.60**	5.77 ± 0.70	**13** (2.36)	**12** (2.18)	**3.6** (0.64)	**12** (2.18)
cis-3-hexenyl isobutyrate	**7.89 ± 0.85**	-	**13** (1.65)	**12** (1.52)	**3.6** (0.30)	**12** (1.52)
cis-3-hexenyl 3-methylbutanoate	**11.94 ± 1.30**	-	**13** (1.09)	**12** (1.01)	**3.6** (0.30)	**12** (1.01)
cis-3-hexenyl hexanoate	**15.34 ± 1.74**	-	**26** (1.16)	**12** (0.78)	**3.6** (0.23)	**12** (0.78)
cis-3-hexenyl *cis*-3-hexenoate	**22.45 ± 2.53**	-	**26** (1.16)	**24** (1.07)	**21.2** (0.94)	**24** (1.07)
cis-3-hexenyl benzoate	**29.11 ± 3.20**	-	**13** (0.45)	**12** (0.41)	**3.6** (0.12)	**12** (0.41)

Atmospheric implications of gas-phase reactions of ozone with cis-3-hexenyl esters

The concentration of atmospheric oxidants, such as hydroxyl radicals (OH), ozone (O_3), and nitrate radicals (NO_3), plays a crucial role in determining the atmospheric lifetime of volatile organic compounds emitted by vegetation. Biogenic emissions of cis-3-hexenyl esters significantly contribute to the global budget of photochemical oxidants and secondary organic aerosols (SOA). The atmospheric degradation of cis-3-hexenyl esters can lead to the formation of carbonyl compounds and acids, such as propanal and propanoic acid, as well as functionalized saturated esters. Understanding the reaction rate constants for the ozonolysis of cis-3-hexenyl esters is essential for comprehending the atmospheric mechanism and its associated implications (Mairean et al., 2025).

The atmospheric lifetime (τ) was calculated for each cis-3-hexenyl ester investigated in these studies, based on the kinetic data obtained and the average concentrations of OH radicals and O_3 during the day. Equations Eq. II.10 and Eq. II.14 were used to calculate the atmospheric lifetime of cis-3-hexenyl esters due to reactions with OH radicals and ozone, respectively, while the overall average atmospheric lifetime (τ_{total}) was estimated using Eq. II.15:

$$\tau_{OH} = 1/k_{(ester+OH)} \times [OH] \quad \text{Eq. II.10}$$

$$\tau_{O3} = 1/k_{(ester+O3)} \times [O_3] \quad \text{Eq. II.14}$$

$$\tau_{total} = 1/\Sigma(k_{(ester+ox)} \times [ox]) \quad \text{Eq. II.15}$$

where $k_{(ester+ox)}$ represents the reaction rate constant of the respective ester with the oxidant species, [ox] (e.g., OH, NO_3, Cl, or O_3), the average concentration of the oxidant species over the course of the day (according to studies), while [ox] is the average atmospheric concentration of the oxidant.

The atmospheric lifetimes of OH-initiated gas-phase reactions for the studied cis-3-hexenyl esters are estimated to range from 2.3 to 7.2 hours, according to the data presented in Table II.14.

The tropospheric lifetime calculated for gas-phase reactions initiated by O_3 with cis-3-hexenyl esters varies between 1.4 and 8.8 hours, as shown in Table II.18.

Table II.18: Tropospheric lifetimes, τ (in hours), for the studied *cis*-3-hexenyl esters with O_3, OH, NO_3, and Cl oxidant species[(a)].

Compound	reaction rate coefficient (cm^3 $molecule^{-1}$ s^{-1})				Tropospheric lifetimes, τ (in hours)				
	$k_{O3} \times 10^{17}$ Mairean et al., 2025	$k_{OH} \times 10^{11}$ Mairean et al., 2024	$k_{NO3} \times 10^{13}$	$k_{Cl} \times 10^{10}$	τ_{O3}	τ_{OH}	τ_{NO3}	τ_{Cl}	τ_{total}
cis-3-hexenyl formate	4.53 ± 0.50	4.13 ± 0.45	-	2.45 ± 0.30 [(c)]	8.8 ± 1.0	6.0 ± 0.7	-	113.4 ± 13.9	< 3.4 ± 0.7
cis-3-hexenyl acetate	5.51 ± 0.60	4.19 ± 0.38	2.46 ± 0.73 [(b)]	-	7.2 ± 0.8	5.9 ± 0.5	2.3 ± 0.7	-	< 1.3 ± 0.2
cis-3-hexenyl isobutyrate	7.89 ± 0.85	4.84 ± 0.39	-	-	5.0 ± 0.5	5.1 ± 0.4	-	-	< 2.5 ± 0.3
cis-3-hexenyl 3-methylbutanoate	11.94 ± 1.30	5.39 ± 0.61	-	-	3.3 ± 0.4	4.6 ± 0.5	-	-	< 1.9 ± 0.3
cis-3-hexenyl hexanoate	15.34 ± 1.74	7.00 ± 0.56	-	-	2.6 ± 0.3	3.5 ± 0.3	-	-	< 1.5 ± 0.2
cis-3-hexenyl *cis*-3-hexenoate	22.45 ± 2.53	10.58 ± 1.40	-	-	1.8 ± 0.2	2.3 ± 0.3	-	-	< 1.0 ± 0.2
cis-3-hexenyl benzoate	29.11 ± 3.20	3.41 ± 0.28	-	-	1.4 ± 0.2	7.2 ± 0.6	-	-	< 1.2 ± 0.2

[(a)] Average tropospheric concentrations used for calculating the lifetimes of cis-3-hexenyl esters: [OH] = $1{,}13\times10^6$ radicals cm^{-3} (Lelieveld et al., 2016); [O_3] = 7×10^{11} molecule cm^{-3} (Logan, 1985); [NO_3] = 5×10^8 radicals cm^{-3} (Shu și Atkinson, 1995); [Cl] = 10^4 atoms cm^{-3} (Wingenter et al., 1999); [(b)] Atkinson et al., 1995; [(c)] Rodríguez et al., 2015; (-) no available data.

III. GENERAL CONCLUSIONS

In this thesis, the rate constants for the gas-phase reactions of seven cis-3-hexenyl esters with OH radicals and ozone were experimentally determined using the relative kinetics method. The experiments were conducted at a standard temperature of (298 ± 2) K and an atmospheric pressure of (1000 ± 10) mbar. The main objectives included determining the photolysis degree, assessing reactivity towards OH radicals and ozone, estimating the mean lifetimes, and evaluating the atmospheric impact of these unsaturated esters.

The studies presented in this thesis for the first time experimentally determined the rate constants for the reactions of five cis-3-hexenyl esters with OH radicals and ozone, and expanded the international kinetic database significantly. These results can form the basis for improving predictive models used in atmospheric chemistry.

The applied relative kinetics method was shown to be effective and robust, yielding reproducible and precise results, consistent with values found in the literature for similar compounds, validating the experimental methodologies used. The experimental conditions were rigorously controlled and verified through a preliminary kinetic study of the reaction between n-butyl acetate and OH radicals, which confirmed the validity of the experimental setup.

The implementation of the "tracer" method to estimate OH radical concentrations in situ proved to be as efficient as traditional approaches using "scavenger" compounds.

The estimated tropospheric mean lifetime for these esters, based on reactions with OH radicals and ozone, is under 8 hours, indicating rapid degradation near biogenic emission sources and a reduced likelihood of long-range transport. Thus, these compounds primarily influence local and regional

photochemical processes, with a direct impact on the budget of photo-oxidants and secondary organic aerosol (SOA) formation.

SELECTIVE BIBLIOGRAPHY

Al Mulla, I., Viera, L., Morris, R., Sidebottom, H., Treacy, J., and Mellouki, A.: Kinetics and Mechanisms for the Reactions of Ozone with Unsaturated Oxygenated Compounds. *ChemPhysChem*, vol. 11, no. 18, pp. 4069–78, https://doi.org/10.1002/cphc.201000404, 2010.

Andreae, M. O., & Merlet, P.: Emission of trace gases and aerosols from biomass burning. *Global Biogeochemical Cycles*, 15(4), 955–966, doi:10.1029/2000gb001382, 2001.

Atkinson, Roger, Carter, W. P. L., Winer, A. M., and Pitts, J. N.: An Experimental Protocol for the Determination of Oh Radical Rate Constants with Organics Using Methyl Nitrite Photolysis as an Oh Radical Source. *Journal of the Air Pollution Control Association*, vol. 31, no. 10, pp. 1090–92, https://doi.org/10.1080/00022470.1981.10465331, 1981.

Atkinson, R., and Carter, W. P. L.: Kinetics and Mechanisms of the Gas-Phase Reactions of Ozone with Organic Compounds under Atmospheric Conditions. *Chemical Reviews*, vol. 84, no. 5, pp. 437–70, https://doi.org/10.1021/cr00063a002, 1984.

Atkinson, Roger, Arey, J., Aschmann, S. M., Corchnoy, S. B., and Shu, Y.: Rate Constants for the Gas-phase Reactions of Cis-3-Hexen-1-ol, Cis-3-Hexenylacetate, Trans-2-Hexenal, and Linalool with OH and NO3 Radicals and O3 at 296 ± 2 K, and OH Radical Formation Yields from the O3 Reactions. *International Journal of Chemical Kinetics*, vol. 27, no. 10, pp. 941–55, https://doi.org/10.1002/kin.550271002, 1995.

Barker, M., Hengst, M., Schmid, J., Buers, H. J., Mittermaier, B., Klemp, D., and Koppmann, R.: Volatile Organic Compounds in the Exhaled Breath of Young Patients with Cystic Fibrosis. *European Respiratory Journal*, vol. 27, no. 5, pp. 929–36, https://doi.org/10.1183/09031936.06.00085105, 2006.

Bejan, I., Barnes, I., Olariu, R., Zhou, S., Wiesen, P., and Benter, T.: Investigations on the Gas-Phase Photolysis and OH Radical Kinetics of Methyl-2-Nitrophenols. *Physical Chemistry Chemical Physics*, vol. 9, no. 42, pp. 5686–92, https://doi.org/10.1039/b709464g, 2007.

Burkholder, J. B., Cox, R. A., and Ravishankara, A. R.: Atmospheric Degradation of Ozone Depleting Substances, Their Substitutes, and Related Species. *Chemical Reviews*, vol. 115, no. 10, pp. 3704–59, https://doi.org/10.1021/cr5006759, 2015.

Calvert, Jack G, Atkinson, R., Becker, K. H., Kamens, R. M., Seinfeld, J. H., Wallington, T. J., and Yarwood, G.: The Mechanisms Of Atmospheric Oxidation Of Aromatic Hydrocarbons. *The Mechanisms Of Atmospheric Oxidation Of Aromatic Hydrocarbons*, https://doi.org/10.1093/oso/9780195146288.001.0001, 2002.

Calvert, Jack G., Orlando, J. J., Stockwell, W. R., and Wallington, T. J.: The Mechanisms of Reactions Influencing Atmospheric Ozone. *The Mechanisms of Reactions Influencing Atmospheric Ozone*,

https://doi.org/10.1093/oso/9780190233020.001.0001, 2015.

Colmenar, I., Martín, P., Cabañas, B., Salgado, S., Tapia, A., and Martínez, E.: Reaction Products and Mechanisms for the Reaction of N-Butyl Vinyl Ether with the Oxidants OH and Cl: Atmospheric Implications. *Atmospheric Environment*, vol. 122, pp. 282–90, https://doi.org/10.1016/j.atmosenv.2015.09.057, 2015.

Fall R.: Biogenic emissions of volatile organic compounds from higher plants. In *Reactive hydrocarbons in the atmosphere*, p. 41-96. Ed. N. Hewitt, London, UK: Academic Press, 1999.

Ferrari, C., Roche, A., Jacob, V., Foster, P., & Baussand, P.: Kinetics of the reaction of OH radicals with a series of esters under simulated conditions at 295 K. *International Journal of Chemical Kinetics,* 28(8), 609–614, doi:10.1002/(sici)1097-4601(1996)28:8<609::aid-kin6>3.0.co;2-z, 1996.

Finlayson-Pitts, B. J. and Pitts, J. N.: Chemistry of the Upper and Lower Atmosphere. *Chemistry of the Upper and Lower Atmosphere*, https://doi.org/10.1016/b978-0-12-257060-5.x5000-x, 2000.

Fortmann, R., Roache, N., Chang, J. C. S., and Guo, Z.: Characterization of Emissions of Volatile Organic Compounds from Interior Alkyd Paint. *Journal of the Air and Waste Management Association*, vol. 48, no. 10, pp. 931–40, https://doi.org/10.1080/10473289.1998.10463741, 1998.

Fraser, M.P., Cass, G.R., Simoneit, B.R.T., Rasmussen, R.A.: Air quality model evaluation data for organics. 5 C6–C22 non-polar and semi-polar aromatic compounds. *Environmental Science and Technology*, 32, 1760–1770, https://doi.org/10.1021/es970349v, 1998.

Graedel, T. E, Hawkins, D. T., Claxton, L. D.: Atmospheric chemical compounds. Sources, occurrence and bioassay, Academic Press Inc.,Orlando, 1986.

Grira, A., Amarandei, C., Roman, C., Bejaoui, O., Aloui, N., El Dib, G., Arsene, C., Bejan, I.G., Olariu, R.I., Canosa, A. and Tomas, A., Gas-Phase Ozone Reaction Kinetics of C5–C8 Unsaturated Alcohols of Biogenic Interest, The Journal of Physical Chemistry A, 126(27), 4413-4423, https://doi.org/10.1021/acs.jpca.2c02805, 2022.

Grosjean, E., & Grosjean, D.: Rate Constants for the Gas Phase Reaction of Ozone with Unsaturated Oxygenates. *International Journal of Chemical Kinetics*, vol. 30, no. 1, pp. 21–29, https://doi.org/10.1002/(SICI)1097-4601(1998)30:1<21::AID-KIN3>3.0.CO;2-W, 1998.

Guenther, A. B., Jiang, X., Heald, C. L., Sakulyanontvittaya, T., Duhl, T., Emmons, L. K., and Wang, X.: The Model of Emissions of Gases and Aerosols from Nature Version 2.1 (MEGAN2.1): An Extended and Updated Framework for Modeling Biogenic Emissions. *Geoscientific Model Development*, vol. 5, no. 6, pp. 1471–92, https://doi.org/10.5194/gmd-5-1471-2012, 2012.

Hartmann, D., Gedra, A., Rhäsa, D., & Zellner, R.: Rate constants for reaction of OH radicals with acetates and glycols in the gas phase. In *Physico-Chemical Behaviour of Atmospheric Pollutants: Proceedings of the Fourth European Symposium held in Stresa, Italy, 23–25 September 1986* (pp. 225-235). Dordrecht: Springer Netherlands, https://doi.org/10.1007/978-94-009-3841-0_25, 1986.

Harvey, R. M., and Petrucci, G. A.: Control of Ozonolysis Kinetics and Aerosol Yield by Nuances in the Molecular Structure of Volatile Organic Compounds. *Atmospheric Environment*, vol. 122, pp. 188–95, https://doi.org/10.1016/j.atmosenv.2015.09.038, 2015.

Hobbs, P. V.: Earth's Atmosphere: Introduction to Atmospheric Chemistry. *Chemistry in Britain*, vol. 37, no. 3, p. 50, 2000.

IPCC2013: CLIMATE CHANGE 2013 Climate Change 2013. *Researchgate.Net*, https://www.researchgate.net/profile/Abha_Chhabra2/publication/271702872_Carbon_and_Other_Biogeochemical_Cycles/links/54cf9ce80cf24601c094a45e/Carbon-and-Other-Biogeochemical-Cycles.pdf, 2013.

Jenkin, M. E., Valorso, R., Aumont, B., Rickard, A. R., and Wallington, T. J.: Estimation of Rate Coefficients and Branching Ratios for Gas-Phase Reactions of OH with Aliphatic Organic Compounds for Use in Automated Mechanism Construction. *Atmospheric Chemistry and Physics*, vol. 18, no. 13, https://doi.org/10.5194/acp-18-9297-2018, 2018a.

Jenkin, M. E., Valorso, R., Aumont, B., Rickard, A. R., & Wallington, T. J.: Estimation of Rate Coefficients and Branching Ratios for Gas-Phase Reactions of OH with Aromatic Organic Compounds for Use in Automated Mechanism Construction. *Atmospheric Chemistry and Physics*, vol. 18, no. 13, pp. 9329–49, https://doi.org/10.5194/acp-18-9329-2018, 2018b.

Jenkin, M. E., Valorso, R., Aumont, B., Newland, M. J., and Rickard, A. R.: Estimation of Rate Coefficients for the Reactions of with Unsaturated Organic Compounds for Use in Automated Mechanism Construction. *Atmospheric Chemistry and Physics*, vol. 20, no. 21, pp. 12921–37, https://doi.org/10.5194/acp-20-12921-2020, 2020.

Keller-Rudek, H., Moortgat, G. K., Sander, R., and Sörensen, R.: The MPI-Mainz UV/VIS Spectral Atlas of Gaseous Molecules of Atmospheric Interest. *Earth System Science Data*, vol. 5, no. 2, pp. 365–73, https://doi.org/10.5194/essd-5-365-2013, 2013.

Kiendler-Scharr, A., Becker, K. H., Doussin, J. F., Fuchs, H., Seakins, P., Wenger, J., and Wiesen, P.: Introduction to Atmospheric Simulation Chambers and Their Applications. In: Doussin, JF., Fuchs, H., Kiendler-Scharr, A., Seakins, P., Wenger, J. (eds) A Practical Guide to Atmospheric Simulation Chambers. Springer, Cham. https://doi.org/10.1007/978-3-031-22277-1_1, 2023.

Kirstine, W., Galbally, I., Ye, Y., and Hooper, M.: Emissions of Volatile Organic Compounds (Primarily Oxygenated Species) from Pasture. *Journal of Geophysical Research: Atmospheres*, vol. 103, no. 3339, pp. 10605–19, https://doi.org/10.1029/97jd03753, 1998.

Kwok, E. S. C., and Atkinson, R.: Estimation of Hydroxyl Radical Reaction Rate Constants for Gas-Phase Organic Compounds Using a Structure-Reactivity Relationship: An Update. *Atmospheric Environment*, vol. 29, no. 14, pp. 1685–95, https://doi.org/10.1016/1352-2310(95)00069-B, 1995.

Lelieveld, J., Gromov, S., Pozzer, A., and Taraborrelli, D.: Global Tropospheric Hydroxyl Distribution, Budget and Reactivity. *Atmospheric Chemistry and Physics*, vol. 16, no. 19, pp. 12477–93, https://doi.org/10.5194/acp-16-12477-2016, 2016.

Logan, J. A.: Tropospheric Ozone: Seasonal Behavior, Trends, and Anthropogenic Influence. *Journal of Geophysical Research*, vol. 90, no. D6, pp. 10463–82, https://doi.org/10.1029/JD090iD06p10463, 1985.

Mairean, C.P., Roman, C., Bejan, I.G., Arsene, C., Olariu, R.I., Gas-phase kinetic study of n-butyl acetate with the OH radicals using the ESC-Q-UAIC facilities chamber, Scientific Communication Session for Undergraduate, Master and PhD Students (SCSSMD) XIth, Iași, Romania, 29-30 October 2020.

Mairean, C. P., Roman, C., Bejan, I. G., Arsene, C., Olariu, R. I.: Gas-phase kinetic study of the OH radicals with some selected cis- 3-hexenyl esters under simulated atmospheric conditions, CNChim2022 XXXVI ed., pp. 214, Călimănești-Căciulata, Romania, 04-07 October 2022a.

Mairean, C. P., Roman, C., Arsene, C., Bejan, I. G., and Olariu, R. I.: Gas-Phase Kinetics of a Series of Cis-3-Hexenyl Esters with OH Radicals under Simulated Atmospheric Conditions. *Journal of Physical Chemistry A*, vol. 128, no. 30, pp. 6274–85, https://doi.org/10.1021/acs.jpca.4c03069, 2024.

Mairean, C. P., Roman, C., Arsene, C., Bejan, I. G., and Olariu, R. I.: Gas-Phase Ozone Reaction Kinetics of a Series of *cis*-3-Hexenyl Esters under Simulated Atmospheric Conditions. *J. Phys. Chem. A 2025,* https://doi.org/10.1021/acs.jpca.5c01004, 2025.

McGillen, M. R., Carey, T. J., Archibald, A. T., Wenger, J. C., Shallcross, D. E., and Percival, C. J.: Structure-Activity Relationship (SAR) for the Gas-Phase Ozonolysis of Aliphatic Alkenes and Dialkenes. *Physical Chemistry Chemical Physics*, vol. 10, no. 13, pp. 1757–68, https://doi.org/10.1039/b715394e, 2008.

McGillen, M. R., Archibald, A. T., Carey, T., Leather, K. E., Shallcross, D. E., Wenger, J. C., and Percival, C. J.: Structure-Activity Relationship (SAR) for the Prediction of Gas-Phase Ozonolysis Rate Coefficients: An Extension towards Heteroatomic Unsaturated Species. *Physical Chemistry Chemical Physics*, vol. 13, no. 7, pp. 2842–49, https://doi.org/10.1039/c0cp01732a, 2011.

Mollner, A. K., Valluvadasan, S., Feng, L., Sprague, M. K., Okumura, M., Milligan, D. B., Bloss, W. J., Sander, S. P., Martien, P. T., Harley, R. A., Mccoy, A. B., and Carter, W. P. L.: Rate of Gas Phase Association Nitrogen Dioxide. *Science*, vol. 646, no. 2010, pp. 646–49, 2010.

Paulson, S. E., Fenske, J. D., Sen, A. D., and Callahan, T. W.: A Novel Small-Ratio Relative-Rate Technique for Measuring OH Formation Yields from the Reactions of O3 with Alkenes in the Gas Phase, and Its Application to the Reactions of Ethene and Propene. *Journal of Physical Chemistry A*, vol. 103, no. 13, pp. 2050–59, https://doi.org/10.1021/jp984140v, 1999.

Peeters, J., Boullart, W., Pultau, V., Vandenberk, S., and Vereecken, L.: Structure-Activity Relationship for the Addition of OH to (Poly)Alkenes: Site-Specific and Total Rate Constants. *Journal of Physical Chemistry A*, vol. 111, no. 9, pp. 1618–31, https://doi.org/10.1021/jp066973o, 2007.

Picquet-Varrault, B., Heroux, S., Chebbi, A., Doussin, J. F., Durand-Jolibois, R., Monod, A., Loirat, H., and Carlier, P.: Kinetics of the Reactions of OH Radicals with Some Oxygenated Volatile Organic Compounds under Simulated Atmospheric Conditions. *International Journal of Chemical Kinetics*, vol. 30, no. 11, pp. 839–47, https://doi.org/10.1002/(SICI)1097-

4601(1998)30:11<839::AID-KIN6>3.0.CO;2-W, 1998.
Ren, Y., Cai, M., Daële, V., and Mellouki, A.: Rate Coefficients for the Reactions of OH Radical and Ozone with a Series of Unsaturated Esters. *Atmospheric Environment*, vol. 200, pp. 243–53, https://doi.org/10.1016/j.atmosenv.2018.12.017, 2019.
Rickard, A. R., Johnson, D., McGill, C. D., and Marslon, G.: OH Yields in the Gas-Phase Reactions of Ozone with Alkenes. *Journal of Physical Chemistry A*, vol. 103, no. 38, pp. 7656–64, https://doi.org/10.1021/jp9916992, 1999.
Rodríguez, D., Rodríguez, A., Bravo, I., Garzón, A., Aranda, A., Diaz-de-Mera, Y., and Notario, A.: Kinetic Study of the Gas-Phase Reactions of Hydroxyl Radicals and Chlorine Atoms with Cis-3-Hexenylformate. *International Journal of Environmental Science and Technology*, vol. 12, no. 9, pp. 2881–90, https://doi.org/10.1007/s13762-014-0686-9, 2015.
Roman, C., Arsene, C., Bejan, I. G., and Olariu, R. I.: Investigations into the Gas-Phase Photolysis and OH Radical Kinetics of Nitrocatechols: Implications of Intramolecular Interactions on Their Atmospheric Behaviour. *Atmospheric Chemistry and Physics*, vol. 22, no. 4, pp. 2203–19, https://doi.org/10.5194/acp-22-2203-2022, 2022.
Shu, Y., and Atkinson, R.: Atmospheric Lifetimes and Fates of a Series of Sesquiterpenes. *Journal of Geophysical Research*, vol. 100, no. D4, pp. 7275–81, https://doi.org/10.1029/95JD00368, 1995.
Sun, S., Cheng, S., and Zhang, H.: Mechanism and Kinetic Study on the Degradation of Unsaturated Esters Initiated by OH Radical. *Theoretical Chemistry Accounts*, vol. 135, no. 6, pp. 1–12, https://doi.org/10.1007/s00214-016-1908-7, 2016.
Taylor, W. D., Allston, T. D., Moscato, M. J., Fazekas, G. B., Kozlowski, R., and Takacs, G. A.: Atmospheric Photodissociation Lifetimes for Nitromethane, Methyl Nitrite, and Methyl Nitrate. *International Journal of Chemical Kinetics*, vol. 12, no. 4, pp. 231–40, https://doi.org/10.1002/kin.550120404, 1980.
Wallington, T. J., Dagaut, P., Liu, R., and Kurylo, M. J.: The Gas Phase Reactions of Hydroxyl Radicals with a Series of Esters over the Temperature Range 240–440 K. *International Journal of Chemical Kinetics*, vol. 20, no. 2, pp. 177–86, https://doi.org/10.1002/kin.550200210, 1988.
Wingenter, O. W., Blake, D. R., Blake, N. J., Sive, B. C., Rowland, F. S., Atlas, E., and Flocke, F.: Tropospheric Hydroxyl and Atomic Chlorine Concentrations, and Mixing Timescales Determined from Hydrocarbon and Halocarbon Measurements Made over the Southern Ocean. *Journal of Geophysical Research Atmospheres*, vol. 104, no. D17, pp. 21819–28, https://doi.org/10.1029/1999JD900203, 1999.
Witte, F., Urbanik, E., and Zetzsch, C.: Temperature Dependence of the Rate Constants for the Addition of OH to Benzene and to Some Monosubstituted Aromatics (Aniline, Bromobenzene, and Nitrobenzene) and the Unimolecular Decay of the Adducts. Kinetics into a Quasi-Equilibrium. 2. *Journal of Physical Chemistry*, vol. 90, no. 14, pp. 3251–59, https://doi.org/10.1021/j100405a040, 1986.
Xing, J. H., Ono, M., Kuroda, A., Obi, K., Sato, K., and Imamura, T.: Kinetic Study of the Daytime Atmospheric Fate of (Z-)-3hexenal. *Journal of Physical*

Chemistry A, vol. 116, no. 33, pp. 8523–29, https://doi.org/10.1021/jp303202h, 2012.

Zhang, Qilei, Lin, X., Gai, Y., Ma, Q., Zhao, W., Fang, B., Long, B., and Zhang, W.: Kinetic and Mechanistic Study on Gas Phase Reactions of Ozone with a Series of: Cis -3-Hexenyl Esters. *RSC Advances*, vol. 8, no. 8, pp. 4230–38, https://doi.org/10.1039/c7ra13369c, 2018.

Zhou, S., Barnes, I., Zhu, T., and Benter, T.: Kinetic Study of Gas-Phase Reactions of OH and NO 3 Radicals and O 3 with Iso-Butyl and Tert-Butyl Vinyl Ethers. *Journal of Physical Chemistry A*, vol. 116, no. 35, pp. 8885–92, https://doi.org/10.1021/jp305992a, 2012.

LIST OF PERSONAL CONTRIBUTIONS INTEGRATED IN THE THESIS

Scientific articles published *in extenso* in journals rated with impact factor in the Web of Science database:

 Mairean C.-P., Roman C., Arsene C., Bejan I.-G., Olariu R.-I., *Gas-Phase Kinetics of a Series of cis-3-Hexenyl Esters with OH Radicals under Simulated Atmospheric Conditions*, *Journal of Physical Chemistry A*, **128**(30), 6274–6285, 2024. https://doi.org/10.1021/acs.jpca.4c03069

Impact Factor: 2.70 – Quartile Q2 (yellow zone).

 Mairean C.-P., Roman C., Arsene C., Bejan I.-G., Olariu R.-I., *Gas-phase ozone reaction kinetics of a series of cis-3-hexenyl esters under simulated atmospheric conditions*, *Journal of Physical Chemistry A*, 2025. https://doi.org/10.1021/acs.jpca.5c01004
Impact Factor: 2.70 – Quartile Q2 (yellow zone).

Participation in Conferences and Scientific Events
Oral Presentations

1. **Mairean C.-P.**, Roman C., Bejan I.-G., Arsene C., Olariu R.-I., *Gas-phase kinetic study of n-butyl acetate with the OH radicals using the ESC-Q-UAIC facilities chamber*, Scientific Communication Session for Undergraduate, Master and PhD Students (SCSSMD), 11th edition, October 29–30, 2020, Iași, Romania.
2. **Mairean C.-P.**, Roman C., Bejan I.-G., Arsene C., Olariu R.-I., *Gas-phase kinetic study of some selected cis-3-hexenyl esters with the OH radicals*, Scientific Communication Session for Undergraduate, Master and PhD Students (SCSSMD), 12th edition, November 11–12, 2021, Iași, Romania.
3. **Măirean C.-P.**, Roman C., Bejan I.-G., Arsene C., Olariu R.-I., *Gas-phase ozonolysis of three cis-3-hexenyl esters under simulated atmospheric conditions*, SCSSMD, 13th edition, page 26, October 28, 2022, Iași, Romania.

Poster Presentation

1. **Mairean C.-P.**, Roman C., Bejan I.-G., Arsene C., Olariu R.-I., *Gas-phase kinetic study of the OH radicals with some selected cis-3-hexenyl esters under simulated atmospheric conditions*, CNChim2022, 36th edition, page 214, October 4–7, 2022, Călimănești-Căciulata, Romania.